Damage to inorganic materials illuminated by focused beam of X-ray free-electron laser radiation

Takahisa Koyama*[a], Hirokatsu Yumoto[a], Kensuke Tono[a], Tadashi Togashi[a], Yuichi Inubushi[a], Tetsuo Katayama[a], Jangwoo Kim[b], Satoshi Matsuyama[b], Makina Yabashi[c], Kazuto Yamauchi[b], Haruhiko Ohashi[a]

[a]Japan Synchrotron Radiation Research Institute (JASRI), 1-1-1 Kouto, Sayo-cho, Sayo-gun, Hyogo 679-5198, Japan

[b]Department of Precision Science & Technology, Graduate School of Engineering, Osaka University, 2-1 Yamadaoka, Suita, Osaka 565-0871, Japan

[c]RIKEN SPring-8 center, 1-1-1 Kouto, Sayo-cho, Sayo-gun, Hyogo 679-5148, Japan

ABSTRACT

X-ray free-electron lasers (XFELs) that utilize intense and ultra-short pulse X-rays may damage optical elements. We investigated the damage fluence thresholds of optical materials by using an XFEL focusing beam that had a power density sufficient to induce ablation phenomena. The 1 μm focusing beams with 5.5 keV and/or 10 keV photon energies were produced at the XFEL facility SACLA (SPring-8 Angstrom Compact free electron LAser). Test samples were irradiated with the focusing beams under normal and/or grazing incidence conditions. The samples were uncoated Si, synthetic silica glass (SiO_2), and metal (Rh, Pt)-coated substrates, which are often used as X-ray mirror materials.

Keywords: X-ray free-electron laser, X-ray mirror, Thin film coating, Ablation, Damage threshold, Focused beam, Hard X-ray

1. INTRODUCTION

With the emergence of X-ray free-electron laser (XFEL) facilities [1, 2], intense ultra-short pulses and fully transverse coherent X-ray pulses have been available in the hard X-ray region. Although XFEL pulses have great capabilities, the intense beams could damage optical elements, which would lead to degradation of the beam quality. Experimentally determined damage thresholds of optical materials are useful for designing XFEL beamline optics such as monochromators, mirrors, focusing optics, slits, and vacuum isolation windows.

Especially in mirror optics, low-Z materials are usually adopted in the coating materials and may also be used in uncoated substrates because of their low absorbance. However, the critical angles of low-Z materials are small, and thus the acceptance apertures of the mirror optics become narrow. As an increasing number of applications demand the use of large mirror apertures, investigation of the damage threshold of metal coatings is required to enlarge the acceptance apertures of mirror optics for high throughput and tight focusing.

In order to investigate the damage thresholds of optical materials, we used focused XFEL pulses that had power densities sufficient to induce ablation phenomena and applied the irradiation under normal and grazing incidence conditions.

The test samples were uncoated Si, synthetic silica glass (SiO_2), and metal (Rh, Pt)-coated substrates for the normal incidence condition, as well as a Rh-coated Si substrate for grazing incidence condition, as these materials are often used in X-ray mirrors.

In the normal incidence condition, the damage thresholds were evaluated by measuring the surface morphology that formed by single-pulse irradiation, with both scanning probe and scanning electron microscopes [3]. In the grazing incidence condition, the damage thresholds were evaluated by measuring the X-ray reflectivity degradation during multiple-pulse irradiation [4].

*koyama@spring8.or.jp; phone +81-791-58-0831; fax +81-791-58-0830

Damage to VUV, EUV, and X-ray Optics V, edited by Libor Juha, Saša Bajt
Richard London, Proc. of SPIE Vol. 9511, 951107 · © 2015 SPIE
CCC code: 0277-786X/15/$18 · doi: 10.1117/12.2182778

2. EXPERIMENTAL SETUP

The schematics of the experimental setup are shown in Figure 1(a). The experiments were performed at Beamline 3 (BL3) of the SACLA [2, 5, 6]. Station 3 of BL3 had a focusing system consisting of a pair of elliptic cylinder mirrors with Kirkpatrick-Baez geometry. These mirrors focused the XFEL beam down to 1 μm (FWHM) at 10 keV [7].

We designed and installed an irradiation chamber dedicated for damage experiments [3]. The irradiation chamber was equipped with precise scan stages for positioning the test sample and measuring the beam profile, optical microscopes with long working distances for online monitoring, and a rotation stage to apply the grazing incidence condition. The surfaces of the samples were monitored by the optical microscope at angles of 30° and 90° for the normal and grazing incidence conditions, respectively.

The irradiation pulse numbers were controlled by using a pulse selector [8]. The pulse energy was controlled by Si and/or Al attenuators of various thicknesses inserted in front of the focusing mirrors. The shot-to-shot fluctuations of the pulse energy were monitored by using a gas monitor (online intensity monitor) [6, 9]. A charge-coupled device (CCD) camera was used for optical aliment of the focusing mirrors.

Focused beam profiles were measured by the knife-edge scanning method after sufficiently reducing the incident pulse energy by using attenuators to avoid inflicting damage on the knife edge. The transmission intensities were measured by a Si PIN photodiode (PD).

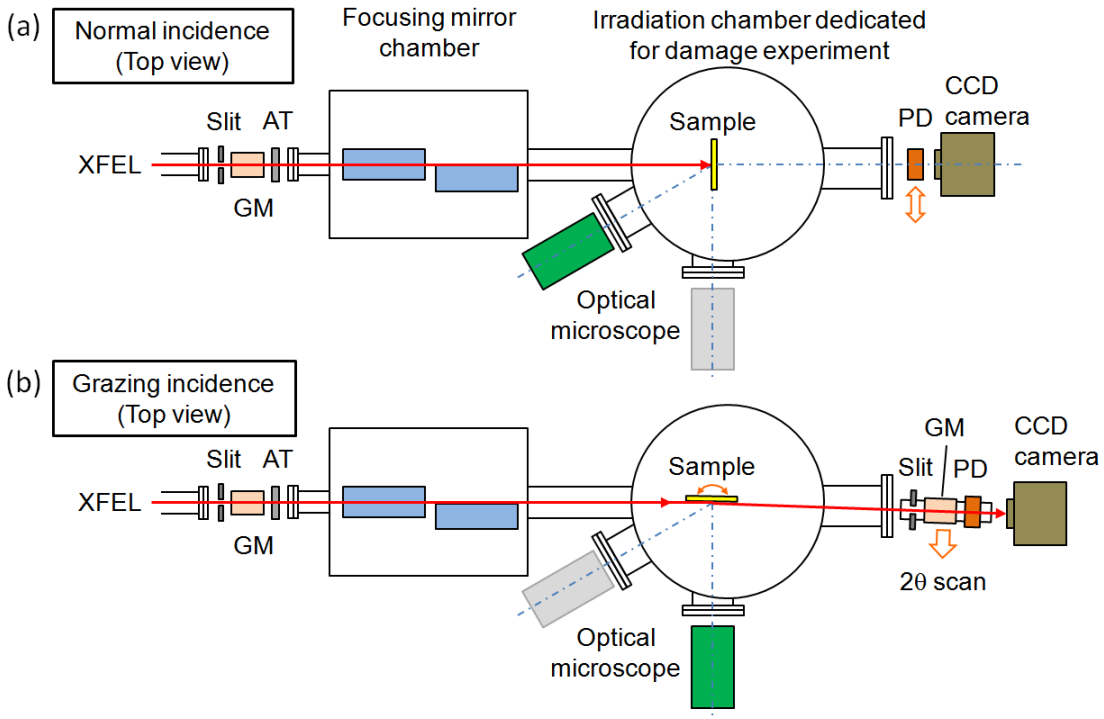

Figure 1. Schematics of experimental setup. (a) Setup for normal incidence condition. (b) Setup for grazing incidence condition. GM: Gas monitor (online intensity monitor), AT: Attenuator, PD: Si PIN photodiode.

In the grazing incidence condition shown in Figure 1(b), the reflectivity of the test sample was measured by using a θ-2θ scan configuration. The reflected beam intensities were measured by using two detectors: an online intensity monitor (gas monitor) was used for high-intensity beams, and a Si PIN photodiode was used for low-intensity beams. A four-quadrant slit, the gas monitor, and the PIN photodiode were mounted on a single optical rail. Two motorized translation stages were used to align the rail position along the axis of the beam reflected from the sample and to enable a θ-2θ scan

with the sample rotation stage. An alignment CCD camera was also used to make the focused beam axis parallel to the sample surface. Figure 2 shows a photograph of the experimental setup for the grazing incidence condition.

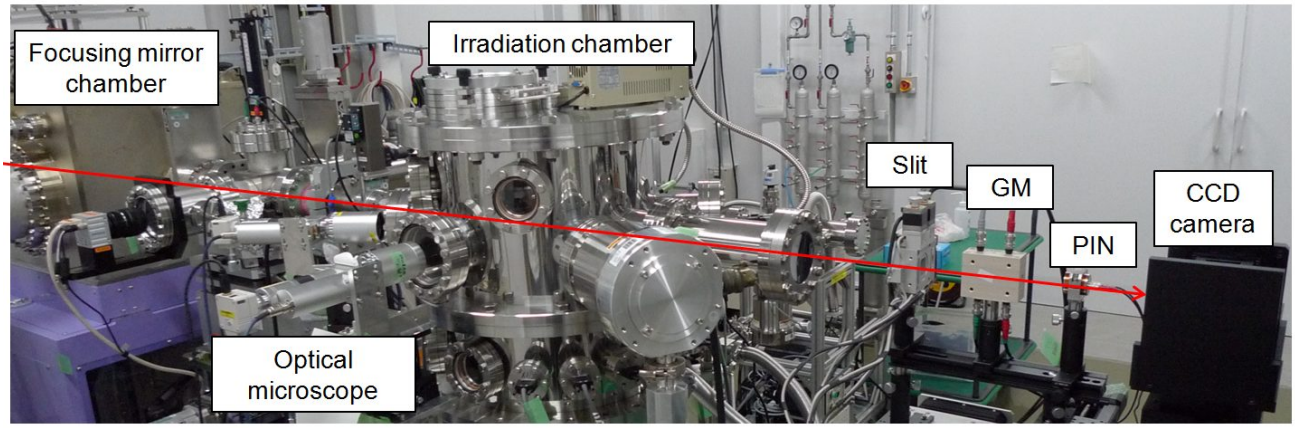

Figure 2. Photograph of experimental setup for grazing incidence condition. XFEL pulses come from left and travel right.

3. RESULTS AND DISCUSSION

3.1 Irradiation under normal incidence condition

In the normal incidence condition, the test samples used were uncoated Si, synthetic silica glass (SiO_2), and metal (Rh, Pt)-coated substrates. During this experiment, the SACLA was operated at a mean pulse energy of 130 μJ, pulse duration of 20 fs [10], and pulse repetition rate of 10 Hz. The X-ray photon energy was selected to be 10 keV.

Figure 3 shows typical single-shot imprints of Si irradiated at high fluence without any attenuators. The sample was moved approximately 3 mm at a speed of 300 μm/s during the exposure. Therefore, 100 imprints were created at 30 μm intervals. The irradiated fluences inside the left, center, and right craters were 33 μJ/μm^2, 36 μJ/μm^2, and 29 μJ/μm^2, respectively. These fluences were several 10s of orders of magnitude higher than the melting dose of Si. Intense spallation and cracks are observed in 10-μm-radius areas on the surface around each crater.

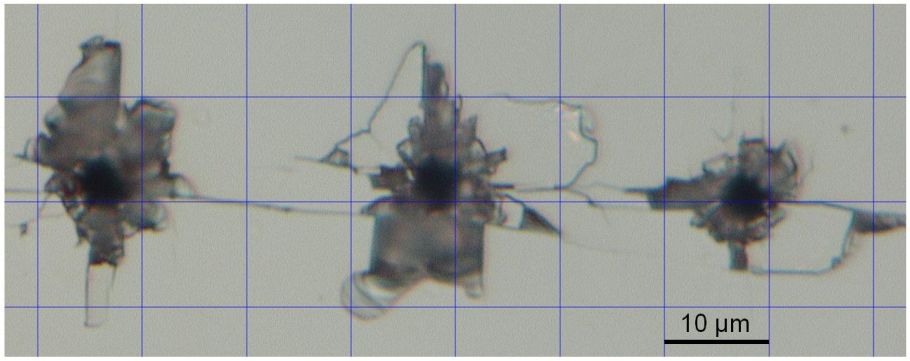

Figure 3. Optical micrograph of silicon surface irradiated with high fluence. Irradiated fluences were 33 μJ/μm^2, 36 μJ/μm^2, and 29 μJ/μm^2 for left, center, and right craters, respectively.

Next, we evaluated the ablation thresholds of the uncoated Si and SiO_2 substrate by varying the intensity using Liu's technique [11]. The typical imprints of uncoated Si and SiO_2 are shown in Figures 4 and 5. The obtained threshold fluences F_{th} were 0.78 μJ/μm^2 (4.5 μJ/μm^2) in Si (SiO_2). Each of these values should be converted to the dose D for a single atom [12-14]. The value of D is given by $D = F_{th}\mu A / (\rho N_A)$, where μ, A, ρ, and N_A are the absorption coefficient, average atomic weight, average density, and Avogadro's constant, respectively. The converted doses were determined to

be 0.73 eV/atom (1.7 eV/atom) in Si (SiO_2). These values reasonably agree with the calculated melting doses of 0.88 eV/atom (1.1 eV/atom) in Si (SiO_2). The melting doses were calculated from the thermodynamic properties [15].

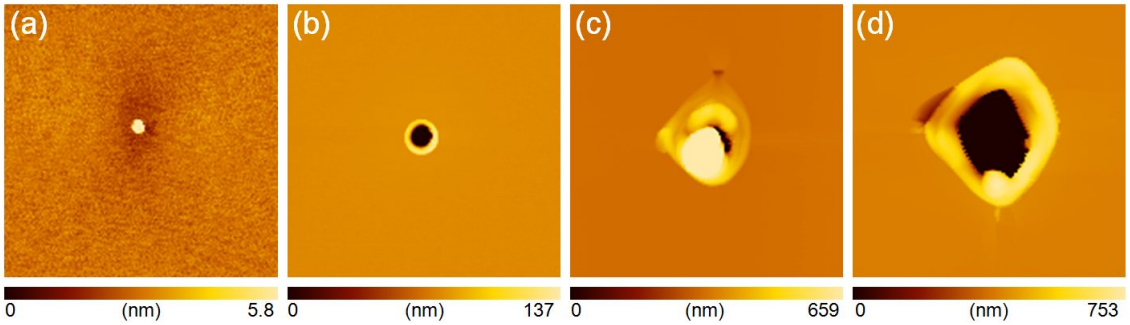

Figure 4. Scanning probe microscope images of uncoated Si. Fluences were (a) 0.9 μJ/μm^2, (b) 1.8 μJ/μm^2, (c) 3.8 μJ/μm^2, and (d) 6.9 μJ/μm^2. Field of view was 6 μm × 6 μm.

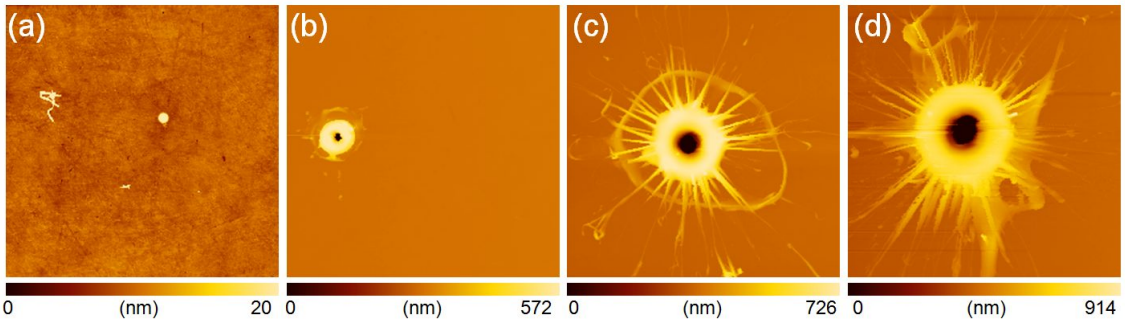

Figure 5. Scanning probe microscope images of uncoated SiO_2. Fluences were (a) 4.7 μJ/μm^2, (b) 5.2 μJ/μm^2, (c) 8.4 μJ/μm^2, and (d) 12 μJ/μm^2. Field of view was 10 μm × 10 μm.

As metal-coated substrates, we used a 200-nm-thick Pt layer coated on Si and SiO_2 substrates. An adhesive layer of 5-nm-thick Cr was inserted. Typical imprints of the Pt-coated SiO_2 substrate are shown in Figure 6. The ablation threshold of the Pt was evaluated to be 0.023 μJ/μm^2 (0.52 eV/atom). This value reasonably agrees with the calculated melting dose of 0.78 eV/atom. However, the ablation threshold of the SiO_2 substrate under the coating layer was evaluated to be 0.11 μJ/μm^2 (0.04 eV/atom), while that of the uncoated SiO_2 substrate was 4.5 μJ/μm^2 (1.7 eV/atom), as stated above. Thus, the threshold value for the coated substrate is 40 times lower than that of the uncoated substrate. Similar results were observed for the Si substrate. Additionally we confirmed similar result using other coating materials, such as Rh. The damage of the substrate underneath the coating could originate from collisions of energetic particles that are generated in the coating region by intense X-rays.

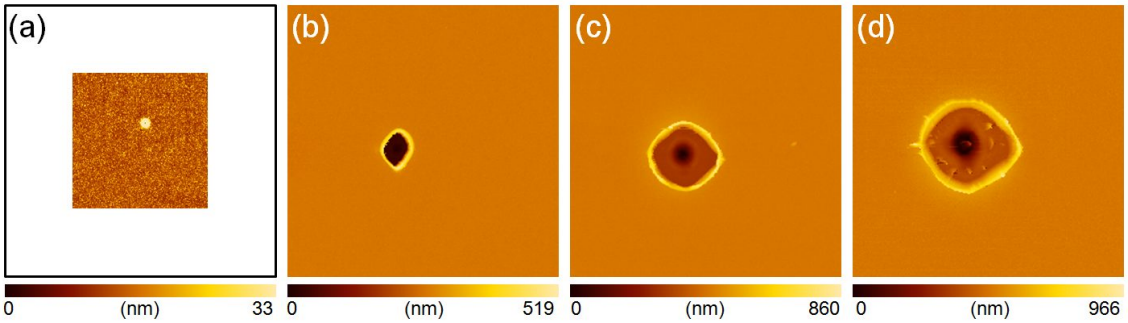

Figure 6. Scanning probe microscope images of uncoated Pt coating on SiO_2 substrate. Fluences were (a) 0.028 μJ/μm^2, (b) 0.15 μJ/μm^2, (c) 0.75 μJ/μm^2, and (d) 1.8 μJ/μm^2. Field of view was 10 μm × 10 μm.

3.2 Irradiation under grazing incidence condition

In the grazing incidence condition, we chose a Rh-coated Si substrate for the test sample. This material is widely used in X-ray mirrors. The coating thickness was 50 nm, and 5-nm-thick Cr was inserted as an adhesive layer. The substrate was 50 mm long, 10 mm wide, and 0.5 mm thick. We selected X-ray photon energies of 5.5 keV and 10 keV. In this paper, the 5.5 keV results are shown. During this experiment, the SACLA was operated with a pulse repetition rate of 30 Hz. Figure 7 shows typical imprints on the Rh-coated Si substrate with a glancing angle of 4.0 mrad. Severe damage occurred at high fluences.

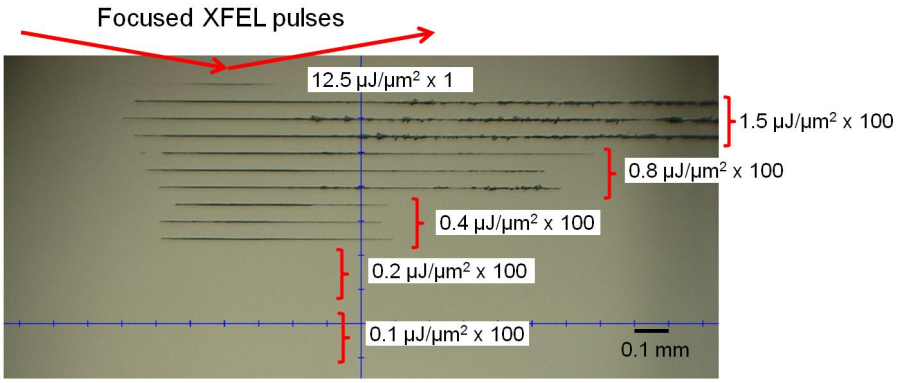

Figure 7. Optical micrograph of Rh-coated Si surface irradiated with various fluences and glancing angle of 4.0 mrad. Fluences and shot numbers are shown in the figure.

Figure 8(a) shows typical reflectivity variations plotted by shot number and with various incident fluences. The glancing angle was 4.0 mrad, and 100 shots were irradiated. The shot-to-shot reflectivity was monitored during irradiation, and damage could occur at the point of reflectivity change. With fluences of 1.55 μJ/μm^2 and 0.78 μJ/μm^2, the reflectivity is observed to drop shortly after the irradiation started, whereas with a fluence of 0.42 μJ/μm^2, the reflectivity drops gradually. No reflectivity changes are observed with the lower fluences.

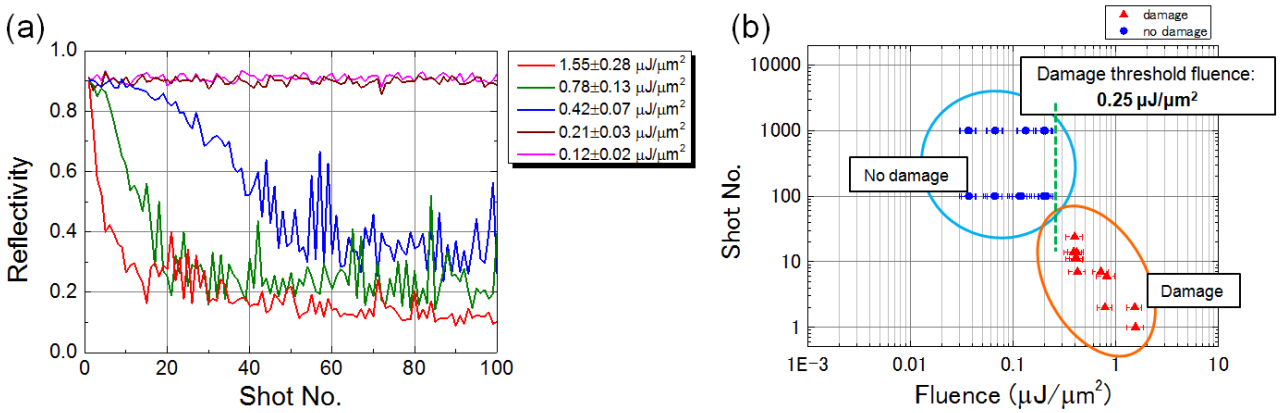

Figure 8. (a) Typical reflectivity variations plotted as function of shot number. (b) Damaged shot numbers plotted as function of fluence. Incident angle was 4.0 mrad.

Figure 8(b) shows the damaged shot numbers plotted as a function of fluence at a glancing angle of 4.0 mrad. The blue circles indicate that no damage was observed in shot numbers 100 or 1000, and the red triangles indicate that damage was observed. The shot numbers plotted are those after the reflectivity changed. The damage fluences were determined by the intermediate value between the damaged and surviving fluences.

Figure 9 shows the damage fluence as a function of the glancing angle. Four of the obtained damage fluences are plotted. At grazing incidence angles of 4.0 mrad, 8.0 mrad, 12.2 mrad, and 24.4 mrad, the measured damage fluences are 0.25 μJ/μm^2, 0.051 μJ/μm^2, 0.013 μJ/μm^2, and 0.014 μJ/μm^2, respectively. The damage fluence curve F_{th} was calculated in the same manner as in [4], in other words, by the function

$$F_{th} = \frac{D_{th}\rho N_A d}{A(1-R)\sin\theta}, \tag{1}$$

where D_{th}, ρ, N_A, A, R, and θ are the threshold dose, density, Avogadro's constant, atomic weight, reflectivity, and incident angle, respectively. The threshold dose D_{th} was measured to be 0.79 eV/atom [3]. The variable d is the energy deposition depth, given by $d = \sqrt{d_x^2 + d_e^2}$, where d_x is the X-ray penetration depth calculated from the absorption coefficient $\mu_g(\theta)$ by

$$\frac{1}{d_x} = \mu_g(\theta) = \frac{2\sqrt{2}\pi}{\lambda}\sqrt{\sqrt{(2\delta-\theta^2)^2+4\beta^2}+2\delta-\theta^2}\ , \tag{2}$$

where the complex refractive index $n = 1 - \delta + i\beta$, and the X-ray wavelength is λ. The variable d_e is the electron collision range [16]. In this case, d_e was assumed to be 10 nm.

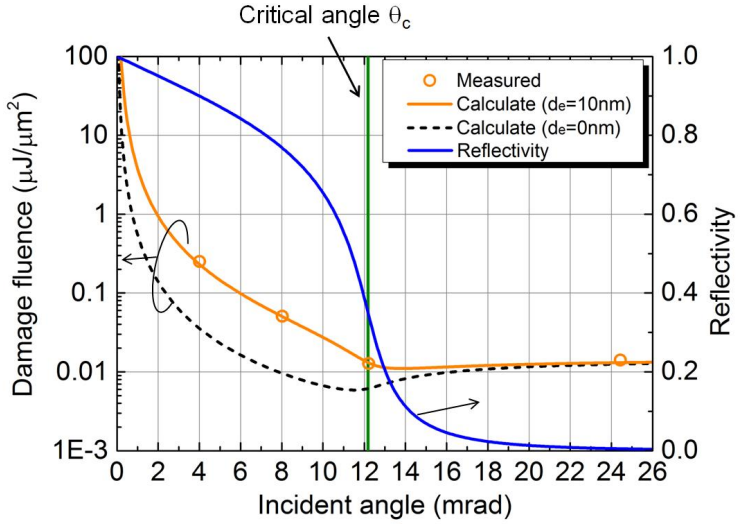

Figure 9. Damage fluence plotted as function of incident angle.

For the practical case using a metal coating at the SACLA, the unfocused beam fluence corresponding to a size of 600 μmϕ (FWHM) and peak pulse energy of 600 μJ at 5.5 keV is on the order of 0.001 μJ/μm^2. This value is one to two orders of magnitude lower than the threshold level. Therefore, a Rh metal coating is usable below the critical angle.

4. SUMMARY

We performed damage measurements of inorganic materials, namely, Si, SiO_2 substrates, and metal-coated substrates, which are often used as X-ray mirror materials. Single- and/or multiple-focused XFEL pulses were irradiated to test the samples under normal and/or grazing incidence conditions, and 1 μm focusing beams with photon energies of 5.5 keV and/or 10 keV were used. In the normal incidence condition, we found that the measured ablation thresholds of uncoated Si and a SiO_2 substrate, as well as metal (Pt and Rh) thin films are comparable to the melting dose, while the substrates under metal-coating layers were easily damaged. In the grazing incidence condition, a Rh-coated Si substrate was tested. The measured damage fluences were significantly higher than the unfocused beam fluence at the SACLA, suggesting that Rh coating is usable in mirror optics at the SACLA.

ACKNOWLEDGMENTS

The authors would like to sincerely thank Takanori Miura for his support in measuring the samples, as well as Hikaru Kishimoto and the SACLA engineering team for their help during the beam time. This work was performed at BL3 of SACLA with the approval of the Japan Synchrotron Radiation Research Institute (JASRI) (Proposal No. 2012A8056, 2012B8052, 2013A8063, and 2014A8051). This research was partially supported by a Grant-in-Aid for Scientific Research (S) (23226004) from the Ministry of Education, Sports, Culture, Science and Technology, Japan (MEXT).

REFERENCES

[1] Emma, P. et al., "First lasing and operation of an ångstrom-wavelength free-electron laser," Nature Photon. 4, 641–647 (2010).
[2] Ishikawa, T. et al., "A compact X-ray free-electron laser emitting in the sub-ångstrom region," Nature Photon. 6, 540–544 (2012).
[3] Koyama, T., Yumoto, H., Senba, Y., Tono, K., Sato, T., Togashi, T., Inubushi, Y., Katayama, T., Kim, J., Matsuyama, S., Mimura, H., Yabashi, M., Yamauchi, K., Ohashi, H., and Ishikawa, T., "Investigation of ablation thresholds of optical materials using 1-μm-focusing beam at hard Xray free electron laser," Opt. Express 21, 15382 (2013).
[4] Koyama, T., Yumoto, H., Tono, K., Sato, T., Togashi, T., Inubushi, Y., Katayama, T., Kim, J., Matsuyama, S., Mimura, H., Yabashi, M., Yamauchi, K., and Ohashi, H., "Damage threshold investigation using grazing incidence irradiation by hard X-ray free electron laser," Proc. SPIE 8848, 88480T (2013).
[5] Tono, K., Inubushi, Y., Sato, T., Togashi, T., Ohashi, H., Kimura, H., Takahashi, S., Takeshita, K., Tomizawa, H., Goto, S., and Yabashi, M., "Beamline for X-ray Free Electron Laser of SACLA," J. Phys. Conference Series 425, 072006 (2013).
[6] Tono, K., Togashi, T., Inubushi, Y., Sato, T., Katayama, T., Ogawa, K., Ohashi, H., Kimura, H., Takahashi, S., Takeshita, K., Tomizawa, H., Goto, S., Ishikawa T., and Yabashi, M., "Beamline, experimental stations and photon beam diagnostics for the hard x-ray free electron laser of SACLA," New J. Phys. 15, 083035 (2013).
[7] Yumoto, H., Mimura, H., Koyama, T., Matsuyama, S., Tono, K., Togashi, T., Inubushi, Y., Sato, T., Tanaka, T., Kimura, T., Yokoyama, H., Kim, J., Sano, Y., Hachisu, Y., Yabashi, M., Ohashi, H., Ohmori, H., Ishikawa, T., and Yamauchi, K., "Focusing of X-ray free electron laser with reflective optics," Nature photon. 7, 43–47 (2013).
[8] Kudo, T., Hirono, T., Nagasono, M., and Yabashi, M., "Vacuum-compatible pulse selector for free-electron laser," Rev. Sci. Instrum. 80, 093301 (2009).
[9] Tono, K., Kudo, T., Yabashi, M., Tachibana, T., Feng, Y., Fritz, D., Hastings, J., and Ishikawa, T., "Single-shot beam-position monitor for x-ray free electron laser," Rev. Sci. Instrum. 82, 023108 (2011).
[10] Inubushi, Y., Tono, K., Togashi, T., Sato, T., Hatsui, T., Kameshima, T., Togawa, K., Hara, T., Tanaka, T., Tanaka, H., Ishikawa, T., and Yabashi, M., "Determination of the pulse duration of an X-ray free electron laser using highly resolved single-shot spectra," Phys. Rev. Lett. 109, 144801 (2012).
[11] Liu, J. M., "Simple technique for measurements of pulsed Gaussian-beam spot sizes," Opt. Lett. 7, 196–198 (1982).
[12] Bionta, R. M., "Controlling dose to low Z solids at LCLS," LCLS Technical Note No. LCLS-TN-00-3 (2000).
[13] London, R. A., Bionta, R. M., Tatchyn, R. O., and Roesler, S., "Computational simulations of high intensity x-ray matter interaction," Proc. SPIE 4500, 51–62 (2001).
[14] Yabashi, M., Higashiya, A., Tamasaku, K., Kimura, H., Kudo, T., Ohashi, H., Takahashi, S., Goto, S., and Ishikawa, T., "Optics development for Japanese XFEL project," Proc. of SPIE 6586, 658605 (2007).
[15] NIST Chemistry WebBook; NIST Standard Reference Database Number 69. http://webbook.nist.gov/chemistry/
[16] Kobetich, E. J., and Katz, R., "Energy Deposition by Electron Beams and δ Rays," Phys. Rev. 170, 391-396 (1968).